JACS
JOURNAL OF THE AMERICAN CHEMICAL SOCIETY
Communication
pubs.acs.org/JACS

Metallophilicity-Driven Dynamic Aggregation of a Phosphorescent Gold(I)–Silver(I) Cluster Prepared by Solution-Based and Mechanochemical Approaches

Wen-Xiu Ni,[†] Yu-Min Qiu,[†] Mian Li,[†] Ji Zheng,[†] Raymond Wai-Yin Sun,[†] Shun-Ze Zhan,[†] Seik Weng Ng,[‡,§] and Dan Li*[,†]

[†]Department of Chemistry and Key Laboratory for Preparation and Application of Ordered Structural Materials of Guangdong Province, Shantou University, Guangdong 515063, PR China

[‡]Department of Chemistry, University of Malaya, 50603 Kuala Lumpur, Malaysia

[§]Chemistry Department, Faculty of Science, King Abdulaziz University, PO Box 80203 Jeddah 21589, Saudi Arabia

Supporting Information

ABSTRACT: We observed an unusual reversible aggregation process showing stimuli-responsive structural dynamics and optical changes attributed to the formation of a sandwich-like Au_3–Ag–Au_3 cluster, which can be synthesized through both solution and mechanochemical methods. Unlike many other heteronuclear gold–silver clusters, the affinity of two cyclic Au_3 complexes and a Ag^I ion is solely bound by ligand unsupported Au–Ag bonding. The assembly/disassembly behavior, further forming nanoaggregates, is controllable by adjusting the concentration of the solution. In the solid state, the insertion of Ag^I ion can be implemented through a mechanochemical approach, accompanied by visual color changes and reversible luminochromism. Furthermore, an uncommon solid–liquid extraction is demonstrated, showing the uniqueness of this labile Au–Ag metallophilicity and hinting at the possibility of manipulating a bonding process through a heterogeneous route.

Gold(I) has a closed-shell d^{10} electronic configuration and often aggregates through noncovalent metal–metal bonding, which has been termed metallophilicity.[1−3] An increasing amount of experimental and theoretical evidence of the metallophilic interactions in gold complexes have provided the basis for dispersion or van der Waals forces enhanced by relativistic effect.[2] Some Au^I complexes are of intense interest because of their unusual phosphorescence properties,[4] which are susceptible to physical or chemical stimuli (mechano-,[5] solvato-,[6] thermo-[7] or vapo-[8] etc.). These stimuli-responsive behaviors are associated with the influence on metal–metal bonding and the corresponding variations of electronic configurations and transitions.

Besides Au^I–Au^I interaction (aurophilicity), gold(I) also exhibits affinity with other closed-shell metals, giving d^{10}–d^{10} or d^{10}–d^8 species.[3] Among these heterometallic complexes, Au^I–Ag^I clusters have attracted recent attentions focusing on their synthesis and promising tunable luminescence.[9] Pyykkö and Laguna reported theoretically heterometallic Au–Ag separation will be shorter than those of homometallic analogues.[2e,10] However, controlling the formation of heterometallic arrays is more difficult than homometallic gold(I) species. Most Au^I–Ag^I clusters are ligand supported.[3a,9] Naumov and Omary proposed that Au–Ag clusters can be conveniently obtained by an acid–base methodology.[11]

Inspired by such a methodology and our previous studies on a family of trinuclear d^{10} coinage-metal clusters,[12] we used a modified trinuclear Au^I-pyrazolate complex (Au_3), whose planar trimeric center is electron-rich and can act as π-base, to attract the acidic Ag^I cation. A phosphorescent sandwich-like cluster, Au_3–Ag–Au_3,[13] is synthesized by both solution and mechanochemical methods. Early works on similar sandwich clusters did not include the study of dynamic behaviors,[13a,b] while recent ones are confined species in coordination cage, organogel or mesoporous silica.[13c−e] In this work, the Au^I–Ag^I bonding undergoes reversible association/dissociation in both solution and solid states, accompanied by optical responses to various stimuli.

The ligand 3-(2-thienyl)-5-phenyl-1*H*-pyrazole (H**L**) reacted with Au(tht)Cl (tht = tetrahydrothiophene) in an acetone/methanol mixed solvent, with the addition of triethylamine, to produce $(Au\mathbf{L})_3$ (see Supporting Information [SI] for experimental details). $(Au\mathbf{L})_3$ exhibits a major absorption peak at 236 nm with a shoulder at 256 nm in CH_2Cl_2 solution (Figure S1 in SI), and shows high-energy emission (λ_{em} 355 nm) in aerated CH_2Cl_2 solution (1×10^{-4} M), consistent with that of H**L**, and a low-energy band (λ_{em} 530 nm) is observed under degassed conditions (Figure S2 in SI). After adding equivalent $AgPF_6$, the colorless solution changed to pale-yellow with a new absorption band growing in the range of 338 to 475 nm (Figure S1 in SI). The critical point for this spectroscopic variation is 1.5×10^{-5} M (denoted C_1), consistent with the concentration-varied excitation spectra (Figure 1c, left), in which, when exceeding C_1, a shoulder at ca. 380 nm first occurred and then predominated. As a result, a strong yellow emission signal (λ_{em} ca. 600 nm) showed up under aerated condition, especially at higher concentrations (up to 1×10^{-3} M, Figure 1c, right), indicating a new species with altered spectroscopic properties is formed.

Received: March 19, 2014
Published: June 18, 2014

dx.doi.org/10.1021/ja5025113 | J. Am. Chem. Soc. 2014, 136, 9532−9535

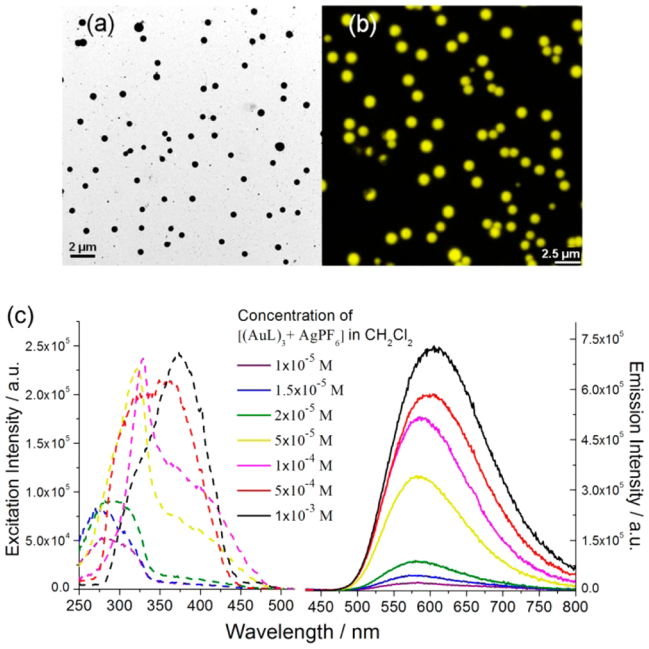

Figure 1. (a) TEM and (b) confocal fluorescence microscopy images of the nanoaggregates formed in the mixture solution of $(AuL)_3$ (1×10^{-3} M) and $AgPF_6$ (5×10^{-4} M) in CH_2Cl_2. (c) Excitation (left, monitored at 600 nm emission) and emission (right) spectra characterizing the dynamic aggregation upon varying concentrations in aerated CH_2Cl_2 solution.

The morphological changes[14] during the aggregation process upon adding $AgPF_6$ was probed by transmission electron microscopy (TEM, Figure 1a), confocal fluorescence microcopy (Figure 1b) and dynamic light scattering (DLS, Figure S3 in SI). It was found that below the concentration of 5×10^{-4} M (denoted C_2), no uniform nanoaggregate formed, whereas at C_2 rather uniform nanodots (diameter ~68 nm) were recorded. Further doubling the concentration to 1×10^{-3} M, the size of the nanodots expanded (diameter ~634 nm). These yellow-emissive nanodots can be observed under confocal fluorescence microcopy (diameter ~700 nm) and TEM (diameter ~ 250 nm due to dried). The size is also dependent on the concentration of Ag^+ (Figure S3 in SI), suggesting the formation of nanoaggregates is related to both the formation of Au–Ag bonds and the solubility of this new heterometallic species. Therefore, at concentrations between C_1 and C_2, the yellow emission came from the Au–Ag clusters formed in solution, while above C_2, the clusters are aggregated and further suspended, enhancing the yellow emission. A slight red shift (13 nm) of the emission peak is also evident above C_2 (Figure 1c, right).

Upon slow crystallization and single-crystal X-ray crystallography (Table S1 in SI), the structure of this new cluster, formulated as $\{Ag[(AuL)_3]_2\}PF_6 \cdot 4CH_2Cl_2$, is revealed (Figure 2a). This Au^I–Ag^I cluster is different from many other ligand supported gold–silver clusters,[3a,9] because a naked Ag^I ion in this cluster is solely bound by six Au^I–Ag^I contacts, giving a sandwich-like distorted trigonal prism. The Au^I–Ag^I distances (2.772(1)–2.831(1) Å, Table S2 in SI), which are close to those of analogous clusters,[13] are even shorter than those in most ligand supported cases.[3a,9] The insertion of Ag^I ion results in the slightly longer intratrimeric Au^I–Au^I distances compared with those in $(AuL)_3$ (Table S3 in SI). DFT and TDDFT calculations (see Computational Section in SI) indicate that the

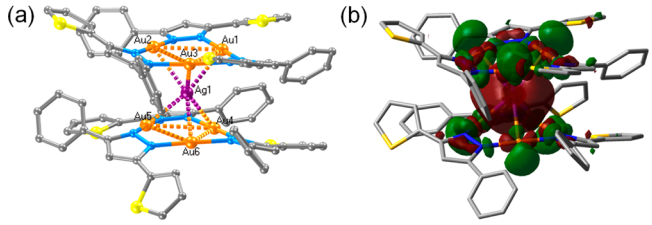

Figure 2. (a) Sandwich-like structure of Au_3–Ag–Au_3. (b) Orbital contour of LUMO (isovalue = 0.02). H atoms, counteranion, solvent molecules, and one set of disorder in the thienyl and phenyl rings are omitted.

orbital energy levels, compositions and electronic transitions are all drastically changed in Au_3–Ag–Au_3 in comparison with those of isolated $(AuL)_3$ and its dimer. In particular, the major absorption transitions of Au_3–Ag–Au_3 are associated with the lowest unoccupied molecular orbital (LUMO, Figure 2b), in which the density is delocalized in the core of the cluster, indicating the major yellow-emissive states originate from the Au^I–Ag^I bonding. The fact that the density in LUMO is protected by the peripheral groups may explain the quenching resistance of Au_3–Ag–Au_3 in aerated solution.[15]

At ambient temperature $\{Ag[(AuL)_3]_2\}PF_6 \cdot 4CH_2Cl_2$ easily lost its crystallized solvent and formed $\{Ag[(AuL)_3]_2\}PF_6$, shown by elemental analysis, IR, UV–vis, ^{1}H NMR spectra and MALDI-TOF mass spectrometry (see SI for details). Interestingly, upon dissolving $\{Ag[(AuL)_3]_2\}PF_6$ in CH_2Cl_2 solution, a reversible dissociation/association process between the Au^I–Ag^I cluster and the isolated $(AuL)_3$ was observed. Such a dynamic process was evidenced by the change of UV–vis spectra (Figure S4 in SI), which showed a decrease of absorption intensity (338–475 nm) upon diluting from 5×10^{-5} to 5×10^{-6} M. Especially at 5×10^{-6} M, the UV–vis spectrum is the same as that of $(AuL)_3$. This conversion is further confirmed by ^{1}H NMR spectra (Figure S5 in SI). In CD_2Cl_2 solution at 1×10^{-3} M, $\{Ag[(AuL)_3]_2\}PF_6$ exhibited broad and poorly resolved NMR signals, indicating the formation of aggregates in the form of heterometallic cluster.[16] In contrast, at 2×10^{-5} M, the NMR signals for the phenyl shifted to downfield, with improved bandwidth and resolution, which are identical with those for $(AuL)_3$. These facts indicate the Au^I–Ag^I bonding can be disconnected merely by diluting the solution. Generally, removal of the bonded Ag^+ ion from heterometallic clusters would require the usage of Cl^- to convert Ag^+ to AgCl.[13c] In this case, the labile, unsupported gold–silver metallophilicity, estimated to be 6–8 kcal mol^{-1},[11] is regarded as arising from nucleophilic or acid–base interaction and behaves like the "loose clusters" described by Vicente and co-workers.[17]

The formation of Au^I–Au^I bonds by mechanochemical route is of considerable interest in the studies of aurophilic interactions.[5] In contrast, the mechanochemical synthesis and mechanochromic property of heterometallic clusters with metallophilicity is rarely explored. Herein, grinding of the white solids of $(AuL)_3$ together with $AgPF_6$ resulted in a change of color to yellow in several minutes, as well as a remarkable luminescence change (Figure 3, top). The soft yellow-green emission (λ_{em} 547 nm) was quickly replaced by a strong yellow one (λ_{em} 602 nm, Figure 3, bottom), which did not occur when grinding $(AuL)_3$ without adding Ag^+. Similar synthetic procedure was also valid when adding $AgNO_3$, $AgBF_4$ or $AgClO_4$ instead of $AgPF_6$, indicating counteranions did not

dx.doi.org/10.1021/ja5025113 | J. Am. Chem. Soc. 2014, 136, 9532–9535

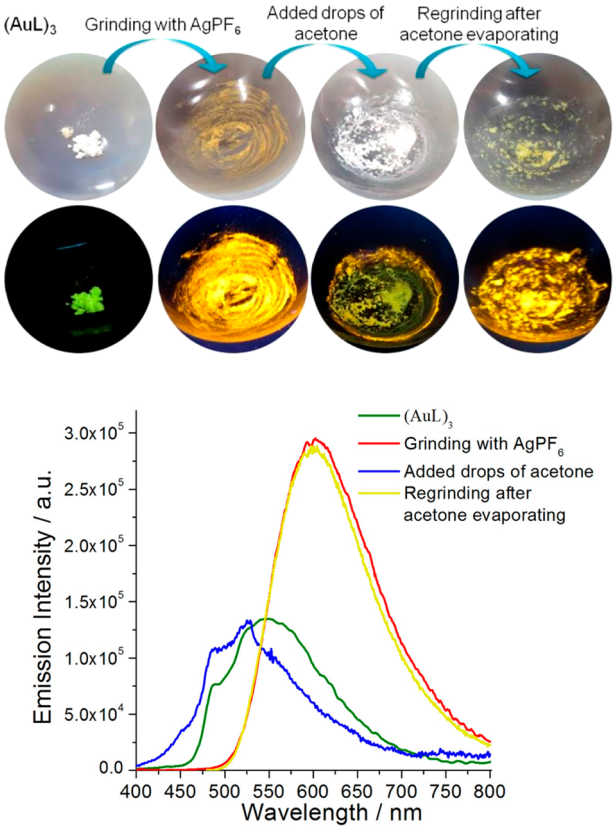

Figure 3. Photographs showing the changes in color (under ambient light) and luminescence (under UV lamp) for the reversible mechanochemical synthesis of $\{Ag[(AuL)_3]_2\}PF_6$ through grinding $(AuL)_3$ with $AgPF_6$ (top), and emission spectra monitoring the reversible mechanochromic procedure upon the excitation of 365 nm (bottom).

influence the process. The mechanochromism here is also reversible upon simply adding a few drops of acetone to the yellow ground powder. The yellow samples reverted to the original white color, and regrinding resulted in the yellow color again, accompanied by reversible changes of visual luminescence and emission spectra recovery (Figure 3). This reversible behavior can also be triggered by the addition of coordinating solvent such as CH_3OH or CH_3CN instead of acetone, while chlorinated solvents such as CH_2Cl_2, $CHCl_3$ or CCl_4 cannot achieve this.

The resultants of the yellow ground Au–Ag mixture were characterized by MALDI-TOF mass spectrometry (Figure S6 in SI). A peak at m/z 1374 corresponding to $\{Ag[(AuL)_3]\}^+$ was found for the ground sample, which is consistent with that of pure $\{Ag[(AuL)_3]_2\}PF_6$. The peak for $\{Ag[(AuL)_3]_2\}^+$ is absent for either the ground sample or the $\{Ag[(AuL)_3]_2\}PF_6$ crystal, probably because part of the labile Au–Ag contacts are broken under laser energy. Therefore, here the Au^I–Ag^I bonds are generated through a mechanical route in the solid state, yielding the heterometallic Au^I–Ag^I structure present in the crystal of $\{Ag[(AuL)_3]_2\}PF_6$. Moreover, the emission profile of the ground sample is identical to that of $\{Ag[(AuL)_3]_2\}PF_6$ (Figure S7 in SI), which displays an intense low-energy structureless emission band (λ_{ex} 440 nm; λ_{em} 602 nm; decay lifetime 6.42 μs; quantum yield 0.21) at room temperature. On the basis of our calculations, the yellow phosphorescence of $\{Ag[(AuL)_3]_2\}PF_6$ originates from the ligand-to-metal–metal (Au–Ag) charge transfer (^{1}LMMCT), which may give rise to the triplet metal-centered (^{3}MM) emissive states (see detailed calculation results in SI).

The fact that the above ground mixtures can rapidly transform from yellow back to white upon adding coordinating solvents indicates the solid–liquid extraction of Ag^+ from this heterometallic cluster is possible. Actually, upon adding CH_3OH, CH_3CN, DMSO or acetone, the yellow crystals of $\{Ag[(AuL)_3]_2\}PF_6$ immediately change to white powders (Figure 4a). In comparison, $\{Ag[(AuL)_3]_2\}PF_6$ is stable in

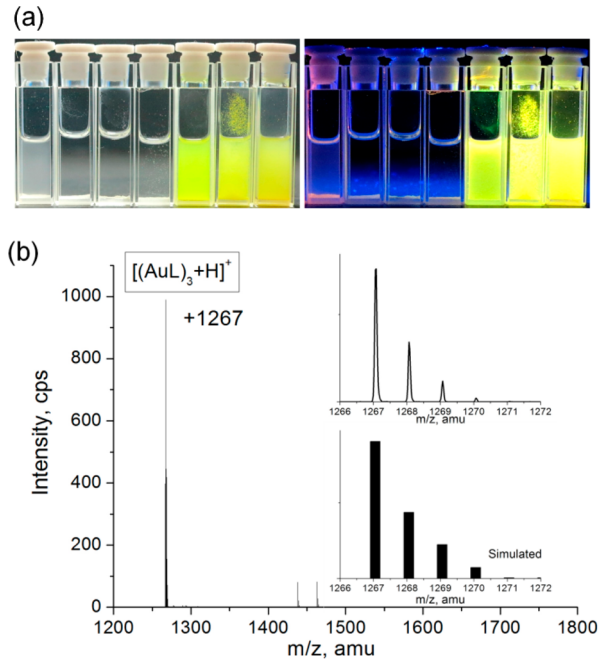

Figure 4. (a) Photographs under ambient light (left) and UV lamp (right) for the crystals of $\{Ag[(AuL)_3]_2\}PF_6$ after adding CH_3OH, CH_3CN, DMSO, acetone, CH_2Cl_2, $CHCl_3$ or CCl_4 (from left to right), respectively. (b) MALDI-TOF mass spectrum of the resulting white powders from the first four cuvettes. Insert: simulated and measured isotopic distribution.

CH_2Cl_2, $CHCl_3$ and CCl_4. The precipitated white powders are confirmed by the MALDI-TOF mass spectrum (Figure 4b, positive mode), which shows a peak at m/z 1267 attributed to $[(AuL)_3 + H]^+$ and a peak for Ag^+ ion at m/z 107 in the solution. Such a heterogeneous dynamics is similar to the process of solid–liquid extraction, but it is unconventional in that there is Au^I–Ag^I bond breaking in this case. More interestingly, during the addition of a few drops of acetone, a simultaneous, dynamic process involving the decomposition of the yellow $\{Ag[(AuL)_3]_2\}PF_6{\cdot}4CH_2Cl_2$ crystals and the fast crystallization of the colorless block-like crystals of $(AuL)_3$ can be real-time recorded within 15 s (see Movie S1 in SI).

In summary, a ligand unsupported heterometallic cluster involving Au^I–Ag^I metallophilic interactions can undergo structural and morphological dynamics, accompanied by visual and spectroscopic response. The reversibility of the mechanochemical synthesis and mechanochromism of this Au^I–Ag^I cluster is attributed to the formation/breaking of the labile Au^I–Ag^I bonding. This work provides a new way to synthesize heterometallic clusters through a simple, economical, and environmentally friendly mechanochemical route. It also exemplifies the elusive nature of metallophilicity, which is

dx.doi.org/10.1021/ja5025113 | J. Am. Chem. Soc. 2014, 136, 9532–9535

generally regarded as weak dispersion force but commonly found strongly phosphorescent, indicative of electronic transition and subsequent intersystem crossing.

■ ASSOCIATED CONTENT

Supporting Information

Experimental details, X-ray crystallographic data, additional physical measurements, figures and descriptions. CCDC 986238−986240. This material is available free of charge via the Internet at http://pubs.acs.org.

■ AUTHOR INFORMATION

Corresponding Author

dli@stu.edu.cn

Notes

The authors declare no competing financial interest.

■ ACKNOWLEDGMENTS

The work was supported by the National Basic Research Program of China (973 Program, Nos. 2013CB834803 and 2012CB821706), and the National Natural Science Foundation of China (Nos. 21171114 and 91222202). W.-X. Ni thanks the funding of China Postdoctoral Science Foundation (No. 2012M521622 and 2013T60811), the Guangdong Natural Science Foundation (No. S2012040006968) and Shantou University. S. W. Ng thanks the funding of the Ministry of Higher Education of Malaysia (Grant No. UM.C/HIR-MOHE/SC/03). We thank Prof. Tai-Chu Lau of City University of Hong Kong for help on physical measurements.

■ REFERENCES

(1) (a) In *Modern Supramolecular Gold Chemistry: Gold-Metal Interactions and Applications*; Laguna, A., Ed.; Wiley-VCH: Weinheim, Germany, 2008; p 347. (b) Yam, V. W.-W.; Cheng, E. C.-C. *Top. Curr. Chem.* **2007**, *281*, 269.

(2) (a) Schmidbaur, H. *Gold Bull.* **1990**, *23*, 11. (b) Schmidbaur, H. *Nature* **2001**, *413*, 31. (c) Schmidbaur, H.; Schier, A. *Chem. Soc. Rev.* **2012**, *41*, 370. (d) Katz, M. J.; Sakai, K.; Leznoff, D. B. *Chem. Soc. Rev.* **2008**, *37*, 1884. (e) Pyykkö, P. *Angew. Chem., Int. Ed.* **2004**, *43*, 4412.

(3) (a) Sculfort, S.; Braunstein, P. *Chem. Soc. Rev.* **2011**, *40*, 2741. (b) Xia, B.-H.; Zhang, H.-X.; Che, C.-M.; Leung, K.-H.; Phillips, D. L.; Zhu, N.; Zhou, Z.-Y. *J. Am. Chem. Soc.* **2003**, *125*, 10362.

(4) (a) Che, C.-M.; Lai, S.-W. In *Gold Chemistry: Luminescence and Photophysics of Gold Complexes*; Mohr, F., Ed.; Wiley-VCH: Weinheim, Germany, 2009; p 249. (b) Yam, V. W.-W.; Lo, K. K. W. *Chem. Soc. Rev.* **1999**, *28*, 323. (c) Yam, V. W.-W.; Cheng, E. C.-C. *Chem. Soc. Rev.* **2008**, *37*, 1806.

(5) (a) Lee, Y. A.; Eisenberg, R. *J. Am. Chem. Soc.* **2003**, *125*, 7778. (b) Seki, T.; Sakurada, K.; Ito, H. *Angew. Chem., Int. Ed.* **1998**, *37*, 2857. (c) Balch, A. L. *Angew. Chem., Int. Ed.* **2009**, *48*, 2641. (d) Ito, H.; Saito, T.; Oshima, N.; Kitamura, N.; Ishizaka, S.; Hinatsu, Y.; Wakeshima, M.; Kato, M.; Tsuge, K.; Sawamura, M. *J. Am. Chem. Soc.* **2008**, *130*, 10044. (e) Ito, H.; Muromoto, M.; Kurenuma, S.; Ishizaka, S.; Kitamura, N.; Sato, H.; Seki, T. *Nat. Commun.* **2013**, *4*, 2009.

(6) (a) Fung, E. Y.; Olmstead, M. M.; Vickery, J. C.; Balch, A. L. *Coord. Chem. Rev.* **1998**, *171*, 151. (b) Chen, K.; Strasser, C. E.; Schmitt, J. C.; Shearer, J.; Catalano, V. J. *Inorg. Chem.* **2012**, *51*, 1207. (c) Mo, L.-Q.; Jia, J.-H.; Sun, L.-J.; Wang, Q.-M. *Chem. Commun.* **2012**, *48*, 8691.

(7) (a) Omary, M. A.; Rawashdeh-Omary, M. A.; Gonser, M. W. A.; Elbjeirami, O.; Grimes, T.; Cundari, T. R. *Inorg. Chem.* **2005**, *44*, 8200. (b) Mohamed, A. A.; Burini, A.; Fackler, J. P., Jr. *J. Am. Chem. Soc.* **2005**, *127*, 5012.

(8) (a) Fernández, E. J.; López-de-Luzuriaga, J. M.; Monge, M.; Olmos, M. E.; Pérez, J.; Laguna, A.; Mohamed, A. A.; Fackler, J. P., Jr. *J. Am. Chem. Soc.* **2003**, *125*, 2022. (b) Lim, A. H.; Olmstead, M. M.; Balch, A. L. *J. Am. Chem. Soc.* **2011**, *133*, 10229. (c) Wenger, O. S. *Chem. Rev.* **2013**, *113*, 3686.

(9) (a) Koshevoy, I. O.; Lin, Y.-C.; Chen, Y.-C.; Karttunen, A. J.; Haukka, M.; Chou, P.-T.; Tunikc, S. P.; Pakkanen, T. A. *Chem. Commun.* **2011**, *47*, 1160. (b) Jia, J.; Wang, Q.-M. *J. Am. Chem. Soc.* **2009**, *131*, 16634. (c) Laguna, A.; Lasanta, T.; López-de-Luzuriaga, J. M.; Monge, M.; Naumov, P.; Olmos, M. E. *J. Am. Chem. Soc.* **2010**, *132*, 456. (d) Jahnke, A. C.; Pröpper, K.; Bronner, C.; Teichgräber, J.; Dechert, S.; John, M.; Wenger, O. S.; Meyer, F. *J. Am. Chem. Soc.* **2012**, *134*, 2938.

(10) Fernández, E. J.; Laguna, A.; López-de-Luzuriaga, J. M.; Monge, M.; Pyykkö, P.; Runeberg, N. *Eur. J. Inorg. Chem.* **2002**, 750.

(11) (a) Tekarli, S. M.; Cundari, T. R.; Omary, M. A. *J. Am. Chem. Soc.* **2008**, *130*, 1669. (b) Lasanta, T.; Olmos, M. E.; Laguna, A.; López-de-Luzuriaga, J. M.; Naumov, P. *J. Am. Chem. Soc.* **2011**, *133*, 16358. (c) Omary, M. A.; Mohamed, A. A.; Rawashdeh-Omary, M. A.; Fackler, J. P., Jr. *Coord. Chem. Rev.* **2005**, *249*, 1372.

(12) (a) Gao, G.-F.; Li, M.; Zhan, S.-Z.; Lv, Z.; Chen, G.-h.; Li, D. *Chem.—Eur. J.* **2011**, *17*, 4113. (b) Zhan, S.-Z.; Li, M.; Zhou, X.-P.; Wang, J.-H.; Yang, J.-R.; Li, D. *Chem. Commun.* **2011**, *47*, 12441. (c) Zhan, S.-Z.; Li, M.; Ng, S. W.; Li, D. *Chem.—Eur. J.* **2013**, *19*, 10217. (d) Ni, W.-X.; Li, M.; Zheng, J.; Zhan, S.-Z.; Qiu, Y.-M.; Ng, S. W.; Li, D. *Angew. Chem., Int. Ed.* **2013**, *52*, 13472.

(13) (a) Burini, A.; Fackler, J. P., Jr.; Galassi, R.; Pietronia, B. R.; Staples, R. J. *Chem. Commun.* **1998**, 95. (b) Burini, A.; Bravi, R.; Fackler, J. P., Jr.; Galassi, R.; Grant, T. A.; Omary, M. A.; Pietronia, B. R.; Staples, R. J. *Inorg. Chem.* **2000**, *39*, 3158. (c) Kishimura, A.; Yamashita, T.; Aida, T. *J. Am. Chem. Soc.* **2005**, *127*, 179. (d) Osuga, T.; Murase, T.; Fujita, M. *Angew. Chem., Int. Ed.* **2012**, *51*, 12199. (e) Lintang, H. O.; Kinbara, K.; Yamashita, T.; Aida, T. *Chem.—Asian J.* **2012**, *7*, 2068.

(14) (a) Po, C.; Tam, A. Y.-Y.; Wong, K. M.-C.; Yam, V. W.-W. *J. Am. Chem. Soc.* **2011**, *133*, 12136. (b) Hu, R.; Leung, N. L. C.; Tang, B. Z. *Chem. Soc. Rev.* **2014**, *43*, 4494.

(15) Cauzzi, D.; Pattacini, R.; Delferro, M.; Dini, F.; Natale, C. D.; Paolesse, R.; Bonacchi, S.; Montalti, M.; Zaccheroni, N.; Calvaresi, M.; Zerbetto, F.; Prodi, L. *Angew. Chem., Int. Ed.* **2012**, *51*, 9662.

(16) (a) Yam, V. W.-W.; Chan, K. H.-Y.; Wong, K. M.-C.; Chu, B. W.-K. *Angew. Chem., Int. Ed.* **2006**, *45*, 6169. (b) Chan, K. H.-Y.; Chow, H. S.; Wong, K. M.-C.; Yeung, M. C.-L.; Yam, V. W.-W. *Chem. Sci.* **2010**, *1*, 477.

(17) Vicente, J.; Chicote, M.-T.; Lagunas, M.-C.; Jones, P. G. *J. Chem. Soc., Chem. Commun.* **1991**, 1730.